IEEE Control Systems Letters paper presented at
2024 IEEE 63rd Conference on Decision and Control (CDC)
December 16-19, 2024. MiCo, Milan, Italy

Distributed Zone Allocation and Preservation in Multiagent Systems*

Deniz Kurtoglu[1], Tansel Yucelen[1], Dzung Tran[2], David Casbeer[2], and Eloy Garcia[2]

***Abstract*— This paper studies the zone allocation and preservation problem in multiagent systems. Specifically, a new state transformation method predicated on a diffeomorphic map is first proposed to make the solution to this problem feasible. Building upon the transformed multiagent system, a new distributed adaptive control protocol is then presented to ensure that an agent approaches a command available to the leader agent(s) when this command enters its zone and otherwise the same agent maintains proximity to this command while preserving its own zone. In addition to the presented system-theoretical results, two illustrative numerical examples are also given to demonstrate the efficacy of the overall architecture.**

I. Introduction

A. Literature Review

Multiagent systems involve groups of agents that fulfill certain collective goals through interacting with each other. Given the potential of these systems across a wide spectrum of civilian and military applications, their significance has notably increased over the last two decades. This growing interest has spurred advancements in distributed control protocols, which are designed to facilitate local interactions among agents. Referenced in seminal works [1]–[4], these protocols employ graph theory to create scalable solutions suitable for even substantially large groups of agents. The reliability of these protocols is also ensured as they are predicated on system-theoretical principles.

Typical distributed control problems involve consensus and bipartite consensus in the leaderless setting (e.g., see [5], [6]), and pinning, containment, and formation in the leader-follower setting (e.g., see [7]–[9]). The common characteristic among these problems is the assumption that agents operate without being subject to specific state constraints. Consequently, they are not directly applicable to the zone allocation and preservation problem. In particular, zone allocation involves assigning specific zones (i.e., state constraints) to each agent, while zone preservation focuses on ensuring that each agent remains within their designated zone throughout the pursuit of a collective goal. A wide spectrum of applications from surveillance and reconnaissance to traffic management and precision agriculture necessitates addressing the zone allocation and preservation problem.

In the literature, there are notable contributions to address the state constraints problem in multiagent systems. For example, barrier functions are utilized by [10], the projection method is applied in [11], and state transformation techniques are employed by [12], [13] to address these constraints in the leaderless setting. However, the operational requirements of certain applications necessitate the leader-follower setting (particularly those involving autonomous mobile robots). In this context, for example, barrier functions are utilized by [14], the projection method is applied in [15], and state transformation strategies are employed in [16], [17] to manage state constraints. While the enforcement of state constraints is important for addressing the zone allocation and preservation problem, the methodologies in [14], [16], [17] presuppose the origin is contained within the state limits. This assumption limits their applicability for scenarios where, for example, a zone strictly within the positive quadrant needs to be assigned to an agent. Therefore, among these contributions, only the approach by [15] and its extensions [18], [19], which do not make this assumption, may be related to the findings of this paper and their relevance is discussed in the next subsection.

B. Contribution

In this paper, we focus on the zone allocation and preservation problem in a leader-following setting, where a bounded time-varying command having a bounded time rate of change is available to the leader agent(s). Specifically, each agent needs to stay at their user-defined heterogeneous zones at all times. As opposed to the methodologies in [14], [16], [17], these zones do not have to contain the origin[1]. Furthermore, a zone of an agent can be intersecting with or disjoint from a zone of any other agent. To this end, a new state transformation method predicated on a monotonically increasing aligned diffeomorphic (mia-diffeomorphic) map is first proposed to make the solution to this problem feasible.

Building upon the transformed multiagent system, a new distributed adaptive control protocol is then presented. In particular, this protocol ensures that an agent approaches a command available to the leader agent(s) when this command enters its zone and otherwise the same agent maintains proximity to this command while preserving its own zone. Here, the adaptive feature of this protocol facilitates operation without the knowledge of an upper bound for the time rate of

*This research was supported by the Air Force Research Laboratory Aerospace Systems Directorate under the Grant FA8650-21-D-2602.

[1]Deniz Kurtoglu and Tansel Yucelen are with the Department of Mechanical Engineering and the Laboratory for Autonomy, Control, Information, and Systems (LACIS, http://lacis.eng.usf.edu/) at the University of South Florida, Tampa, Florida 33620, United States of America (emails: denizkurtoglu@usf.edu, yucelen@usf.edu).

[2]Dzung Tran, David Casbeer, and Eloy Garcia are with the Air Force Research Laboratory, Control Science Center, Wright-Patterson Air Force Base, Ohio 45433, United States of America (emails: dzung.tran.ctr@afrl.af.mil, david.casbeer@us.af.mil, eloy.garcia.2@us.af.mil).

[1]The result documented in Section III-A of this paper, which is predicated on Definition 2 below, may facilitate the extension of the methodologies in [16], [17] to address the zone allocation and preservation problem.

change of the command. In addition to the presented system-theoretical results, two illustrative numerical examples are also given to demonstrate the efficacy of the overall architecture. Finally, although the scope and methodology of the approach by [15] and its extensions [18], [19] differ from those of this paper, they may offer a potential solution for the zone allocation and preservation problem. Nonetheless, their applicability is not limited only to constant command(s) but also may necessitate additional assumptions beyond those made in this paper (e.g., Assumption 3 of [15], Assumption 2 of [18], and Assumption 2 of [19]).

II. Mathematical Preliminaries

A. Notation

In this paper, the sets of real number numbers, positive real numbers, and nonnegative real numbers are respectively denoted as $\mathbb{R}$, $\mathbb{R}_+$, and $\overline{\mathbb{R}}_+$; the sets of $n\times m$ real matrices, $n\times n$ positive-definite real matrices, and $n\times n$ nonnegative-definite real matrices are respectively denoted as $\mathbb{R}^{n\times m}$, $\mathbb{R}_+^{n\times n}$, and $\overline{\mathbb{R}}_+^{n\times n}$; and vector of all zeros and all ones are respectively denoted as $\mathbf{0}_n$ and $\mathbf{1}_n$. Furthermore, we use $(\cdot)^{\mathrm{T}}$ for transpose, $(\cdot)^{-1}$ for inverse, $|\cdot|$ for absolute value, $\|\cdot\|_1$ for 1-norm, $\|\cdot\|_2$ for 2-norm, and "$\triangleq$" for equality by definition. For a vector $a=[a_1,a_2,\ldots,a_n]^{\mathrm{T}}$, we also use $\mathrm{Sgn}(a)\triangleq[\mathrm{sgn}(a_1),\ldots,\mathrm{sgn}(a_n)]^{\mathrm{T}}$ and $\mathrm{Tanh}(a)\triangleq[\tanh(a_1),\ldots,\tanh(a_n)]^{\mathrm{T}}$, where $\mathrm{sgn}(\cdot)$ and $\tanh(\cdot)$ respectively denote signum and tangent hyperbolic functions.

The graph-theoretical notation utilized in this paper is now introduced. Specifically, an undirected graph is represented by $\mathcal{G}$, which is characterized by the node set $\mathcal{V}_{\mathcal{G}}=\{1,\ldots,n\}$ and the edge set $\mathcal{E}_{\mathcal{G}}\subset\mathcal{V}_{\mathcal{G}}\times\mathcal{V}_{\mathcal{G}}$ with an edge $(i,j)\in\mathcal{E}_{\mathcal{G}}$ indicating that nodes i and j are neighbors ($i\sim j$ signifies neighboring relation herein). A graph $\mathcal{G}$ is also considered connected when a finite path $i_0i_1\ldots i_L$ exists with $i_{k-1}\sim i_k$ and $k=1,\ldots,L$ between any two distinct nodes. Furthermore, the degree matrix for $\mathcal{G}$ is defined as $\mathcal{D}(\mathcal{G})\triangleq\mathrm{diag}(d)$, where $d=[d_1,\ldots,d_n]^{\top}$ and d_i being the number of the neighbors of node i. The adjacency matrix for $\mathcal{G}$ is also defined as $\mathcal{A}(\mathcal{G})\in\mathbb{R}^{n\times n}$, where $[\mathcal{A}(\mathcal{G})]_{ij}=1$ when $(i,j)\in\mathcal{E}_{\mathcal{G}}$ and $[\mathcal{A}(\mathcal{G})]_{ij}=0$ otherwise. The Laplacian matrix for $\mathcal{G}$ is now defined as $\mathcal{L}(\mathcal{G})\triangleq\mathcal{D}(\mathcal{G})-\mathcal{A}(\mathcal{G})$. Finally, let $\mathcal{K}=\mathrm{diag}\,(k)$, $k=[k_1,\ldots,k_n]^{\mathrm{T}}$, $k_i\in\overline{\mathbb{R}}_+$, and assume that at least one k_i is nonzero. Then, $\mathcal{F}(\mathcal{G})\triangleq\mathcal{L}(\mathcal{G})+\mathcal{K}\in\mathbb{R}_+^{n\times n}$ holds for a fixed, connected, and undirected $\mathcal{G}$ [3, Lemma 3.3], where we consider such a $\mathcal{G}$ in this paper.

B. Diffeomorphism

A diffeomorphic map $\phi(x)$ is an isomorphic relationship between smooth manifolds, where its definition is now given.

Definition 1. A map $\phi:\mathcal{S}\to\mathcal{T}$ between two differentiable manifolds $\mathcal{S}$ and $\mathcal{T}$ is called a diffeomorphic map if it is a bijection and both $\phi(x)$ and its inverse $\phi^{-1}:\mathcal{T}\to\mathcal{S}$ are continuously differentiable.

Some examples to diffeomorphic maps include $\phi(x)=3x+2$ with $\mathcal{S}=(0,1)$ and $\mathcal{T}=(2,5)$, $\phi(x)=\mathrm{atanh}(x)$ with $\mathcal{S}=(-1,1)$ and $\mathcal{T}=\mathbb{R}$ [20], and rotation of the plane with $\mathcal{S}\in\mathbb{R}^2$ and $\mathcal{T}\in\mathbb{R}^2$. Yet, we need to define a new diffeomorphic map $\phi(x)$ for the results presented in this paper. For this purpose, let $x_i\in\mathcal{S}_i$ be the state of an agent i, where $\mathcal{S}_i=(\underline{x}_i,\bar{x}_i)\subset\mathbb{R}$ such that $\underline{x}_i<\bar{x}_i$. Let also $\mathcal{T}_i=\mathbb{R}$ for all agents. We are now ready to give the next definition.

Definition 2. A map $\phi_i:\mathcal{S}_i\to\mathbb{R}$ between two differentiable manifolds $\mathcal{S}_i$ and $\mathbb{R}$ is called a monotonically increasing aligned diffeomorphic (mia-diffeomorphic) map if it satisfies the following conditions:

i) $\phi_i(x_i)$ is a diffeomorphic map.
ii) $\phi_i(x_i)$ is monotonically increasing subject to $\lim_{x_i\to\underline{x}_i}\phi_i(x_i)=-\infty$, $\lim_{x_i\to\bar{x}_i}\phi_i(x_i)=\infty$, $\lim_{x_i\to\underline{x}_i}\phi_i'(x_i)=\infty$, and $\lim_{x_i\to\bar{x}_i}\phi_i'(x_i)=\infty$, where $\phi_i'\triangleq\mathrm{d}\phi_i/\mathrm{d}x_i$.
iii) $\phi_i(x_i)=x_i$ over $x_i\in\mathcal{U}_i\subset\mathcal{S}_i$.

The last item in Definition 2 means that $\phi_i(x_i)$ aligns with the identity line (i.e., the line having a unity slope and no bias) over $x_i\in\mathcal{U}_i$. One can readily obtain a mia-diffeomorphic map by constructing a composite function, which is discussed in the next remark.

Remark 1. For a given $\mathcal{S}_i=(\underline{x}_i,\bar{x}_i)$, let $\mathcal{U}_i=(\underline{x}_i+\delta_i,\bar{x}_i-\delta_i)$ with $\delta_i\in(0,(\bar{x}_i-\underline{x}_i)/2)$. One can then obtain a mia-diffeomorphic map $\phi_i:\mathcal{S}_i\to\mathbb{R}$ using a line and an inverse hyperbolic tangent through the composite function

$$\phi_i(x_i)=\begin{cases}f_i(x_i), & x_i\in(\underline{x}_i,\underline{x}_i+\delta_i/\kappa_i)\cup(\bar{x}_i-\delta_i/\kappa_i,\bar{x}_i),\\ x_i, & x_i\in\mathcal{U}_i,\\ g_{1i}(x_i), & x_i\in[\underline{x}_i+\delta_i/\kappa_i,\underline{x}_i+\delta_i],\\ g_{2i}(x_i), & x_i\in[\bar{x}_i-\delta_i,\bar{x}_i-\delta_i/\kappa_i],\end{cases}\tag{1}$$

where $f_i(x_i)\triangleq\xi_{1i}^{-1}\mathrm{atanh}(\xi_{1i}(x_i-\xi_{2i}))+\xi_{2i}$, $\xi_{1i}=2/(\bar{x}_i-\underline{x}_i)$, $\xi_{2i}=(\bar{x}_i+\underline{x}_i)/2$, $g_{1i}\triangleq m_{0i}+m_{1i}x_i+m_{2i}x_i^2+m_{3i}x_i^3$, $g_{2i}\triangleq m_{4i}+m_{5i}x_i+m_{6i}x_i^2+m_{7i}x_i^3$, and $\kappa_i>1$. In (1), $g_{1i}(x_i)$ and $g_{2i}(x_i)$ are active over the transition area, where $m_{li}\in\mathbb{R}$, $l=0,\ldots,7$, are determined through solving the boundary expressions given by $g_{1i}(\underline{x}_i+\delta_i/\kappa_i)=f_i(\underline{x}_i+\delta_i/\kappa_i)$, $g_{1i}'(\underline{x}_i+\delta_i/\kappa_i)=f_i'(\underline{x}_i+\delta_i/\kappa_i)$, $g_{1i}(\underline{x}_i+\delta_i)=\underline{x}_i+\delta_i$, $g_{1i}'(\underline{x}_i+\delta_i)=1$, $g_{2i}(\bar{x}_i-\delta_i)=\bar{x}_i-\delta_i$, $g_{2i}'(\bar{x}_i-\delta_i)=1$, $g_{2i}(\bar{x}_i-\delta_i/\kappa_i)=f_i(\bar{x}_i-\delta_i/\kappa_i)$, and $g_{2i}'(\bar{x}_i-\delta_i/\kappa_i)=f_i'(\bar{x}_i-\delta_i/\kappa_i)$ with $g_{1i}'\triangleq\mathrm{d}g_{1i}/\mathrm{d}x_i$, $g_{2i}'\triangleq\mathrm{d}g_{2i}/\mathrm{d}x_i$, and $f_i'\triangleq\mathrm{d}f_i/\mathrm{d}x_i$. Note that these expressions make $\phi_i(x_i)$ continuous and continuously differentiable. Figure 1 illustrates the resulting mia-diffeomorphic map $\phi_i(x_i)$ given by (1).

III. Problem Definition

We focus on a multiagent system with n agents that exchange information over a fixed, connected, and undirected graph $\mathcal{G}$. A subset of these agents referred to as leader agent(s) has access to a bounded time-varying command $c(t)$ having a bounded time rate of change, whereas those without access are referred to as follower agent(s). Mathematically speaking, the single-integrator dynamics of agent i, $i=1,\ldots,n$, has the form given by

$$\dot{x}_i(t)=u_i(t),\quad x_i(0)=x_{i0},\tag{2}$$

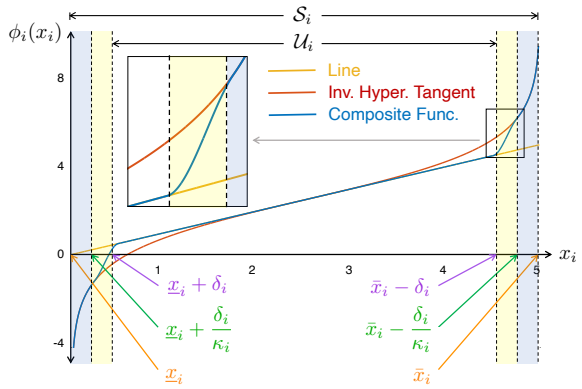

Fig. 1. A mia-diffeomorphic map is constructed as a composite function using a line and an inverse hyperbolic tangent, where the yellow highlighted region denotes the transition area ($\underline{x}_i = 0$, $\bar{x}_i = 5$, $\delta_i = 0.5$, and $\kappa_i = 2$).

where $x_i(t)$ and $u_i(t)$ respectively represent the state and control signal of this agent. At this point, we are ready to define the zone allocation and preservation problem.

Definition 3. Given a user-defined heterogeneous zone $\mathcal{S}_i = (\underline{x}_i, \bar{x}_i) \subseteq \mathbb{R}$, $\underline{x}_i < \bar{x}_i$, for agent i, $i = 1, \ldots, n$, the zone allocation and preservation problem is to determine $u_i(t) \in \mathbb{R}$ such that the following conditions hold:

i) $\lim_{t\to\infty}\big(x_i(t) - c(t)\big) = 0$ when $c(t) \in \mathcal{U}_i$.

ii) $x_i(t) \in \mathcal{S}_{\mathrm{d}i}$ when $c(t) \in \mathcal{S}_{\mathrm{d}i}$ or $c(t) \notin \mathcal{S}_i$, where $\mathcal{S}_{\mathrm{d}i} \triangleq \mathcal{S}_i \setminus \mathcal{U}_i$ is a disjoint set and the state $x_i(t)$ belongs to either the left side or the right side of this set whichever is closer to the command $c(t)$.

Remark 2. Definition 3 implies that the state of each agent remains within its user-defined heterogeneous zone at all times. It also implies that the state of an agent does not move to an arbitrary point within its zone. Instead, it either approaches the command when $c(t) \in \mathcal{U}_i$ and otherwise it maintains proximity to the command (see Figure 2a), where "proximity" here is explicitly defined by the second item in Definition 3.

Remark 3. While we consider a one-dimensional setting for the system-theoretical results presented in this paper, they can be applied to multiple dimensions for agent dynamics having the form $\dot{x}_i^j(t) = u_i^j(t)$ with j being the dimension index. We refer to Section V for two illustrative numerical examples in a two-dimensional setting (see also Figure 2b on an interpretation of Definition 3 in such a setting).

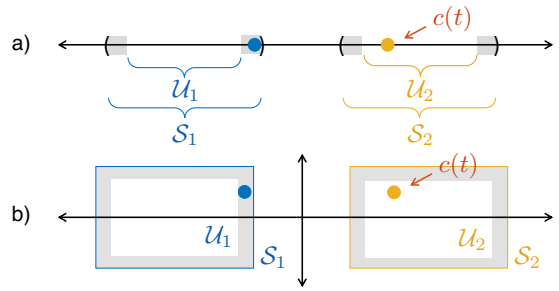

Fig. 2. Demonstration of Definition 3 for two agents depicted in both **a)** one-dimensional and **b)** two-dimensional settings, where the gray highlighted regions denote $\mathcal{S}_{\mathrm{d}i}$. The blue and yellow dots respectively represent the states $x_1(t)$ and $x_2(t)$. The command $c(t)$ stays in $\mathcal{S}_2$ in this demonstration that yields $x_2(t) = c(t)$.

For the solvability of the problem defined in Definition 3, the following assumption is necessary.

Assumption 1. Initial conditions of the states of all agents satisfy $x_{i0} \in \mathcal{S}_i$.

As the zone allocation and preservation problem is defined, the rest of this section first focuses on a new state transformation method and then presents a new proposed distributed adaptive control protocol.

A. State Transformation

We now introduce a state transformation to convert the constrained state $x_i(t) \in \mathcal{S}_i$ to an unconstrained counterpart $z_i(t) \in \mathbb{R}$. For this purpose, consider a mia-diffeomorphic map $\phi_i : \mathcal{S}_i \to \mathbb{R}$ given in Definition 2. Consider also $z_i(t) \triangleq \phi_i(x_i(t))$ that yields

$$\dot{z}_i(t) = \big(\partial\phi_i(x_i(t))/\partial x_i(t)\big)u_i(t) \tag{3}$$

for each agent. Next, let the control signal be

$$u_i(t) = \big(\partial\phi_i(x_i(t))/\partial x_i(t)\big)^{-1} v_i(t) \tag{4}$$

with $v_i(t) \in \mathbb{R}$ being the virtual control signal, which yields

$$\dot{z}_i(t) = v_i(t), \quad z_i(0) = \phi_i(x_i(0)). \tag{5}$$

Remark 4. The above state transformation and control signal selection yield to the following observations:

i) (5) represents an unconstrained single-integrator dynamics of agent i, $i = 1, \ldots, n$.

ii) From Definition 2, the term $\big(\partial\phi_i(x_i(t))/\partial x_i(t)\big)^{-1}$ in (4) vanishes at the boundary $\partial\mathcal{S}_i$ of the user-defined heterogeneous zones for each agent. Hence, if $v_i(t)$ is bounded, then $\lim_{x_i(t)\to\partial\mathcal{S}_i} u_i(t) = 0$.

iii) From Definition 2, $z_i(t) = x_i(t)$ over $x_i(t) \in \mathcal{U}_i$.

The second and third observations in Remark 4 play a key role in addressing the problem in Definition 3, where we refer to Theorem 2 in Section IV on this point.

B. Distributed Adaptive Control Protocol

We now introduce the proposed distributed adaptive control protocol. For this purpose, consider the virtual control signal of agent i, $i = 1, \ldots, n$, given by

$$\begin{aligned} v_i(t) = &-\alpha_i\Big(\sum_{i\sim j}(z_i(t) - z_j(t)) + k_i(z_i(t) - c(t))\Big) \\ &-\hat{\beta}_i(t)\mathrm{sgn}\Big(\sum_{i\sim j}(z_i(t) - z_j(t)) + k_i(z_i(t) - c(t))\Big), \end{aligned} \tag{6}$$

where $\alpha_i \in \mathbb{R}_+$ and $\hat{\beta}_i(t)$ is the adaptive term updated according to

$$\dot{\hat{\beta}}_i(t) = \gamma_i\Big|\sum_{i\sim j}(z_i(t) - z_j(t)) + k_i(z_i(t) - c(t))\Big| \tag{7}$$

with $\gamma_i \in \mathbb{R}_+$. In (6) and (7), $k_i = 1$ for leader agents and otherwise $k_i = 0$.

Remark 5. In (6), if one replaces $\hat{\beta}_i(t)$ with a constant, then that constant must be chosen to be equal to or larger

than an upper bound for the time rate of change of the command (e.g., see [9], [21]). Hence, the purpose of the adaptive term (7) is to enable the operation of the proposed protocol without prior knowledge of such an upper bound.

To address the problem in Definition 3, the next section shows that the error signals

$$e_i(t) = z_i(t) - c(t), \tag{8}$$

of each agent asymptotically approach zero in the unconstrained domain. For the actual constrained domain involving the heterogeneous zones of each agent, it corresponds to an agent approaching a command when this command enters its zone and otherwise the same agent maintains proximity to this command while preserving its zone.

IV. System-Theoretical Analysis

We are now ready to present the system-theoretical analysis of the proposed architecture. To this end, by adding and subtracting $c(t)$ in (6), and using (5), the time derivative of this error $e_i(t)$ yields

$$\begin{aligned}\dot{e}_i(t) = &-\alpha_i\Big(\sum_{i\sim j}(e_i(t)-e_j(t)) + k_i e_i(t)\Big)\\ &-\hat{\beta}_i(t)\mathrm{sgn}\Big(\sum_{i\sim j}(e_i(t)-e_j(t)) + k_i e_i(t)\Big) - \dot{c}(t),\\ &e_i(0) = e_{i0}. \end{aligned}\tag{9}$$

Next, let $e(t) \triangleq [e_1(t),\ldots,e_n(t)]^{\mathrm{T}}$, $\mathcal{A} = \mathrm{diag}([\alpha_1,\ldots,\alpha_n]^{\mathrm{T}})$, $\hat{\mathcal{B}}(t) = \mathrm{diag}([\hat{\beta}_1(t),\ldots,\hat{\beta}_n(t)]^{\mathrm{T}})$, $\mathcal{F}(\mathcal{G}) \triangleq \mathcal{L}(\mathcal{G}) + \mathcal{K} \in \mathbb{R}_+^{n\times n}$ with $\mathcal{L}(\mathcal{G})$ being the Laplacian matrix for a fixed, connected, and undirected graph $\mathcal{G}$, and $\mathcal{K} = \mathrm{diag}\,(k)$ with $k = [k_1,\ldots,k_n]^{\mathrm{T}}$. The compact form of (9) can then be written as

$$\dot{e}(t) = -\mathcal{A}\mathcal{F}e(t) - \hat{\mathcal{B}}(t)\mathrm{Sgn}(\mathcal{F}e(t)) - \mathbf{1}_n\dot{c}(t). \tag{10}$$

The following two theorems present the main contributions of this paper.

Theorem 1. Consider the transformed multiagent system consisting of n agents over a fixed, connected, and undirected graph $\mathcal{G}$ with dynamics given by (5) subject to Assumption 1. Then, the virtual control signals given by (6) and (7) yield $\lim_{t\to\infty} e_i(t) = 0$ for all agents.

Proof. Consider the energy function

$$\mathcal{V}(\cdot) = \frac{1}{2}e^{\mathrm{T}}\mathcal{F}e + \frac{1}{2\gamma_i}\sum_{i=1}^{n}\tilde{\beta}_i^2, \tag{11}$$

where $\tilde{\beta}_i(t) = \hat{\beta}_i(t) - \bar{\dot{c}}$ with $\bar{\dot{c}}$ being the upper bound of the time derivative of the command $c(t)$. The time-derivative of (11) satisfies

$$\begin{aligned}\dot{\mathcal{V}}(\cdot) \;=\; &-e^{\mathrm{T}}(t)\mathcal{F}\mathcal{A}\mathcal{F}e(t) - e^{\mathrm{T}}(t)\mathcal{F}\hat{\mathcal{B}}(t)\mathrm{Sgn}(\mathcal{F}e(t))\\ &-e^{\mathrm{T}}(t)\mathcal{F}\mathbf{1}_n\dot{c}(t) + \frac{1}{\gamma_i}\sum_{i=1}^{n}\tilde{\beta}_i(t)\dot{\hat{\beta}}_i(t).\end{aligned}\tag{12}$$

Note that $-e^{\mathrm{T}}(t)\mathcal{F}\hat{\mathcal{B}}(t)\mathrm{Sgn}(\mathcal{F}e(t))$ in (12) can be written in the form given by

$$\begin{aligned}&-e^{\mathrm{T}}(t)\mathcal{F}\hat{\mathcal{B}}(t)\mathrm{Sgn}(\mathcal{F}e(t))\\ &\qquad = -\sum_{i=1}^{n}\hat{\beta}_i(t)\Big|\sum_{i\sim j}(e_i(t)-e_j(t)) + k_i e_i(t)\Big|\end{aligned}\tag{13}$$

and $-e^{\mathrm{T}}(t)\mathcal{F}\mathbf{1}_n\dot{c}(t)$ in (12) can be upper bounded as

$$\begin{aligned}-e^{\mathrm{T}}(t)\mathcal{F}\mathbf{1}_n\dot{c}(t) &\le |e^{\mathrm{T}}(t)\mathcal{F}|_1\bar{\dot{c}}\\ &= \sum_{i=1}^{n}\Big|\sum_{i\sim j}(e_i(t)-e_j(t)) + k_i e_i(t)\Big|\bar{\dot{c}}.\end{aligned}\tag{14}$$

Using (13) and (14) in (12) and $\dot{\tilde{\beta}}_i(t) = \dot{\hat{\beta}}_i(t)$, one can obtain

$$\begin{aligned}\dot{\mathcal{V}}(\cdot) \le &-e^{\mathrm{T}}(t)\mathcal{F}\mathcal{A}\mathcal{F}e(t) - \sum_{i=1}^{n}\hat{\beta}_i(t)\Big|\sum_{i\sim j}(e_i(t)-e_j(t))\\ &+k_i e_i(t)\Big| + \sum_{i=1}^{n}\Big|\sum_{i\sim j}(e_i(t)-e_j(t)) + k_i e_i(t)\Big|\bar{\dot{c}}\\ &+\frac{1}{\gamma_i}\sum_{i=1}^{n}\tilde{\beta}_i(t)\dot{\hat{\beta}}_i(t)\\ \le &-e^{\mathrm{T}}(t)\mathcal{F}\mathcal{A}\mathcal{F}e(t) - \Big(\sum_{i=1}^{n}\tilde{\beta}_i(t)\Big)\Big|\sum_{i\sim j}(e_i(t)-e_j(t))\\ &+k_i e_i(t)\Big| + \frac{1}{\gamma_i}\sum_{i=1}^{n}\tilde{\beta}_i(t)\dot{\hat{\beta}}_i(t).\end{aligned}\tag{15}$$

Adding and subtracting $c(t)$ to (7), using the resulting expression in (15), and since $\mathcal{F}\mathcal{A}\mathcal{F} \in \mathbb{R}_+^{n\times n}$, we arrive

$$\dot{\mathcal{V}}(\cdot) \le -e^{\mathrm{T}}(t)\mathcal{F}\mathcal{A}\mathcal{F}e(t) \le 0. \tag{16}$$

Hence, the pair $(e_i(t), \tilde{\beta}_i(t))$ is bounded for all agents. From [22, Theorem 2], it can now be concluded that the right-hand side of (16) approaches zero asymptotically, where this implies that $\lim_{t\to\infty} e_i(t) = 0$ for all agents. ■

Note that the above theorem extends beyond the scope of problem addressed in this paper, which offers applicability to unconstrained distributed control problems within a leader-follower framework. Building upon the results of Theorem 1, the next theorem shows that the proposed overall architecture solves the problem in Definition 3.

Theorem 2. Consider a multiagent system consisting of n agents over a fixed, connected, and undirected graph $\mathcal{G}$ with dynamics given by (2) subject to Assumption 1. Then, the proposed overall architecture given by (4), (6), and (7) solves the problem in Definition 3.

Proof. Over the unconstrained domain $z_i(t) \in \mathbb{R}$ represented by (5), it is proven in Theorem 1 that each agent asymptotically follows the command $c(t)$. Over the constrained domain $x_i(t) \in \mathcal{S}_i$ represented by (2), we are now ready to show what this implies:

- *i)* If $c(t) \in \mathcal{U}_i$ for agent i, then $\lim_{t\to\infty}\big(x_i(t) - c(t)\big) = 0$ since $\lim_{t\to\infty} e_i(t) = 0$ by Theorem 1 and $z_i(t) = x_i(t)$ over $x_i(t) \in \mathcal{U}_i$ by Definition 2.
- *ii)* If $c(t) \in \mathcal{S}_{\mathrm{d}i}$ or $c(t) \notin \mathcal{S}_i$ for agent i, then $x_i(t) \in \mathcal{S}_{\mathrm{d}i}$. The former case, when $c(t) \in \mathcal{S}_{\mathrm{d}i}$, holds since the

state $x_i(t)$ of this agent must enter $\mathcal{S}_{\mathrm{d}i}$ owing to the fact that the term $\big(\partial\phi_i(x_i(t))/\partial x_i(t)\big)^{-1}$ in its control signal (4) is unity at the boundary $\partial\mathcal{U}_i$. The latter case, when $c(t) \notin \mathcal{S}_i$, also holds since its virtual control signal (6) is bounded by Theorem 1 and the term $\big(\partial\phi_i(x_i(t))/\partial x_i(t)\big)^{-1}$ in its control signal (4) vanishes at the boundary $\partial\mathcal{S}_i$ of its zone by Definition 2, which together yields $\lim_{x_i(t)\to\partial\mathcal{S}_i} u_i(t) = 0$ (i.e., the state $x_i(t)$ of this agent cannot leave $\mathcal{S}_i$). Finally, since $\mathcal{S}_{\mathrm{d}i}$ is a disjoint set, this further implies for the latter case that the state $x_i(t)$ of this agent practically stops moving at either the left side or the right side of this set, whichever is closer to the command $c(t)$ (i.e., $x_i(t)$ maintains proximity to $c(t)$ when $c(t) \notin \mathcal{S}_i$).

This shows that the proposed overall architecture given by (4), (6), and (7) solves the problem in Definition 3. ■

Remark 6. While the state $x_i(t)$ of agent i can follow the command $c(t)$ to some extent when $c(t) \in \mathcal{S}_{\mathrm{d}i}$ and $c(t)$ stays close to the boundary $\partial\mathcal{U}_i$, this may not hold when $c(t) \in \mathcal{S}_{\mathrm{d}i}$ and $c(t)$ stays close to the boundary $\partial\mathcal{S}_i$. This issue can practically be addressed through enlarging the domain $\mathcal{U}_i$ (e.g., through decreasing δ_i in Remark 1).

V. Illustrative Numerical Examples

We now provide two illustrative numerical examples to demonstrate the efficacy of the overall architecture. Before presenting these examples, we would like to state the following remark.

Remark 7. We would like to highlight two observations that need to be considered in the practical applications of the proposed architecture. First, it is common practice to approximate $\mathrm{sgn}(x)$ in (6) with $\tanh(\rho x)$ with $\rho \in \mathbb{R}_+$ being a large constant to avoid the chattering phenomenon in the control signals of each agent. Second, the adaptive term of each agent given by (7) can take large numbers since its right hand side is always a nonnegative quantity. To mitigate this situation, a leakage term can be introduced as follows

$$\dot{\hat{\beta}}_i(t) \;=\; \gamma_i\Big|\sum_{i\sim j}(z_i(t)-z_j(t)) + k_i(z_i(t)-c(t))\Big| - \sigma_i\hat{\beta}_i(t) \tag{17}$$

with $\sigma_i \in \mathbb{R}_+$ being sufficiently small. Despite these modifications, the efficacy of the proposed architecture remains sufficiently close to its original one.

Two examples are now ready to be given in a two-dimensional setting. To this end, subscripts "x" and "y" are added to the related signals to clarify the distinction between the two axes. In the first example, let the first agent have access to the command given by $c_{\mathrm{x}}(t) = 1.75\sin(0.05t)+2$ and $c_{\mathrm{y}}(t) = 1.75\cos(0.05t)+2$ over $t \in [0, 120]$. Here, the user-defined zones $\mathcal{S}_i = [\underline{x}_{\mathrm{x}i}, \bar{x}_{\mathrm{x}i}, \underline{x}_{\mathrm{y}i}, \bar{x}_{\mathrm{y}i}]$ of each agent are chosen as $\mathcal{S}_1 = [2,4,2,4]$, $\mathcal{S}_2 = [2,4,0,2]$, $\mathcal{S}_3 = [0,2,0,2]$, $\mathcal{S}_4 = [0,2,2,4]$. In addition, the initial conditions $(x_{\mathrm{x}i}(0), x_{\mathrm{y}i}(0))$ of agents are respectively chosen $(3,3)$, $(3,1)$, $(1,1)$, and $(1,3)$ to satisfy Assumption 1. We also use the mia-diffeomorphic map given by (1) with

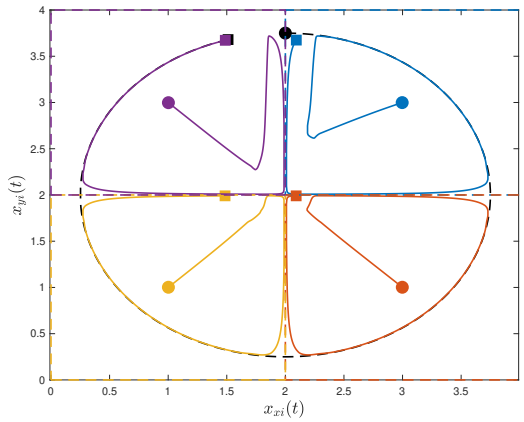

Fig. 3. Closed-loop multiagent response with the proposed architecture, where solid blue, orange, yellow, and purple lines respectively indicate agents 1, 2, 3, and 4, and the black dashed line indicates the command. The circle and the square markers respectively represent the initial position and the final position.

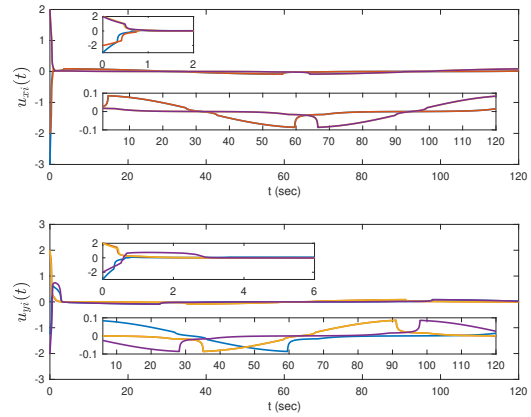

Fig. 4. Control histories of the proposed architecture, where the top and bottom figures respectively show the control signal for each agent along the x-axis and the y-axis.

$\delta_i = 0.3$ and $\kappa_i = 3$ for all agents. Finally, we choose $\alpha_i = 1$ for (6), $\gamma_i = 1$ and $\sigma_i = 0.01$ for (17) in view of Remark 7, and use $\tanh(\rho x)$ with $\rho = 50$ instead of $\mathrm{sgn}(x)$ also in view of Remark 7. Figure 3 shows the closed-loop multiagent system response, whereas Figure 4 shows the corresponding control histories. From these figures, it is clear that all agents approach the command when this command is in their zones and otherwise they maintain proximity to this command while preserving their zones.

In the second example, let the first agent have access to the command given by $c_{\mathrm{x}}(t) = 2\sin(0.05t)+2$ and $c_{\mathrm{y}}(t) = t/20$ over $t \in [0, 120]$. Here, the user-defined zones $\mathcal{S}_i = [\underline{x}_{\mathrm{x}i}, \bar{x}_{\mathrm{x}i}, \underline{x}_{\mathrm{y}i}, \bar{x}_{\mathrm{y}i}]$ of each agent are chosen as $\mathcal{S}_1 = [0,3,2,6]$, $\mathcal{S}_2 = [0,3,0,5]$, $\mathcal{S}_3 = [1,4,2,6]$, $\mathcal{S}_4 = [2,4,0,5]$. In addition, the initial conditions $(x_{\mathrm{x}i}(0), x_{\mathrm{y}i}(0))$ of agents are respectively chosen $(1,3)$, $(2,1)$, $(2.5,4)$, and $(3,2)$ to satisfy Assumption 1. All the remaining parameters are chosen identical to the first example. Figure 5 shows the individual closed-loop multiagent system responses, whereas Figure 6 shows the corresponding control histories. Once again, from these figures, it is clear that all agents approach

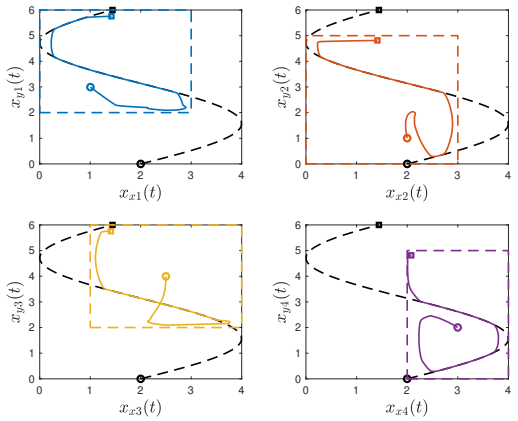

Fig. 5. Individual closed-loop agent responses with the proposed architecture, where solid blue, orange, yellow, and purple lines respectively indicate agents 1, 2, 3, and 4, and the black dashed line indicates the command. The circle and the square markers respectively represent the initial position and the final position.

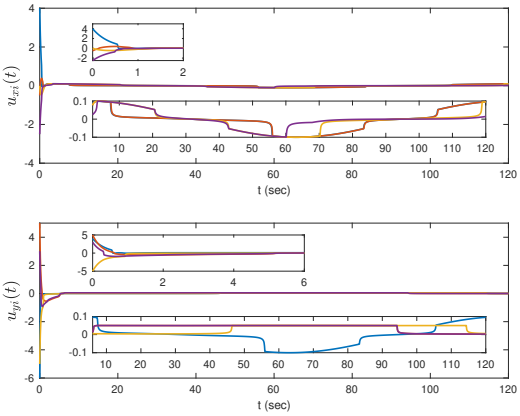

Fig. 6. Control histories of the proposed architecture, where the top and bottom figures respectively show the control signal for each agent along the x-axis and the y-axis.

the command when this command is in their zones and otherwise they maintain proximity to this command while preserving their zones.

VI. Conclusion

The zone allocation and preservation problem in multiagent systems (see Definition 3) was addressed in this paper. Predicated on a mia-diffeomorphic map (see Definition 2), a new state transformation was first used to convert the constrained states of agents, resulting from user-defined heterogeneous zones, to their unconstrained counterpart (see Section III-A). Subsequently, a new distributed adaptive control protocol was proposed within a leader-follower setting (see Section III-B). Notably, it was shown in Theorems 1 and 2 (see Section IV) that the overall architecture solves the zone allocation and preservation problem. This was achieved by ensuring an agent approaches a command available to the leader agents(s) when this command enters its zone and otherwise the same agent maintains proximity to this command while preserving its own zone. Two illustrative numerical examples were also provided (see Section V) to showcase the efficacy of this architecture. Future research can include, first, extensions of the overall framework to agents having high-order dynamics, and second, agents that are subject to exogenous disturbances and/or system uncertainties.

References

[1] W. Ren and R. W. Beard, *Distributed consensus in multi-vehicle cooperative control*. Springer, 2008, vol. 27, no. 2.

[2] M. Mesbahi and M. Egerstedt, *Graph theoretic methods in multiagent networks*. Princeton University Press, 2010.

[3] F. L. Lewis, H. Zhang, K. Hengster-Movric, and A. Das, *Cooperative control of multi-agent systems: Optimal and adaptive design approaches*. Springer Science & Business Media, 2013.

[4] F. Bullo, *Lectures on network systems*. Kindle Direct Publishing Seattle, DC, USA, 2020, vol. 1, no. 3.

[5] R. Olfati-Saber, J. A. Fax, and R. M. Murray, "Consensus and cooperation in networked multi-agent systems," *Proceedings of the IEEE*, vol. 95, no. 1, pp. 215–233, 2007.

[6] C. Altafini, "Consensus problems on networks with antagonistic interactions," *IEEE Transactions on Automatic Control*, vol. 58, no. 4, pp. 935–946, 2012.

[7] Q. Song, J. Cao, and W. Yu, "Second-order leader-following consensus of nonlinear multi-agent systems via pinning control," *Systems and Control Letters*, vol. 59, no. 9, pp. 553–562, 2010.

[8] M. Ji, G. Ferrari-Trecate, M. Egerstedt, and A. Buffa, "Containment control in mobile networks," *IEEE Transactions on Automatic Control*, vol. 53, no. 8, pp. 1972–1975, 2008.

[9] D. Tran, T. Yucelen, and E. L. Pasiliao, "Formation control with multiplex information networks," *IEEE Transactions on Control Systems Technology*, vol. 28, no. 2, pp. 462–476, 2018.

[10] W. Xiao, L. Cao, G. Dong, W. Bai, and Q. Zhou, "Adaptive consensus control for stochastic nonlinear multiagent systems with full state constraints," *International Journal of Robust and Nonlinear Control*, vol. 30, no. 4, pp. 1487–1511, 2020.

[11] G. Wang and Z. Zuo, "Consensus control of multi-agent systems with different state constraints and event-triggered communication," *IEEE Transactions on Circuits and Systems II: Express Briefs*, 2023.

[12] W. Meng, Q. Yang, J. Si, and Y. Sun, "Consensus control of nonlinear multiagent systems with time-varying state constraints," *IEEE Transactions on Cybernetics*, vol. 47, no. 8, pp. 2110–2120, 2016.

[13] F. Yuan, J. Lan, Y. Liu, and L. Liu, "Adaptive nn control for nonlinear multi-agent systems with unknown control direction and full state constraints," *IEEE Access*, vol. 9, pp. 24 425–24 432, 2020.

[14] J. Fu, G. Wen, and X. Yu, "Safe consensus tracking with guaranteed full state and input constraints: A control barrier function based approach," *IEEE Transactions on Automatic Control*, 2023.

[15] P. Lin, G. Li, and K. Huang, "Position-constrained containment for second-order discrete-time multi-agent systems," *Systems and Control Letters*, vol. 142, p. 104708, 2020.

[16] Q. Ji, G. Chen, and Q. He, "Neural network-based distributed finite-time tracking control of uncertain multi-agent systems with full state constraints," *IEEE Access*, vol. 8, pp. 174 365–174 374, 2020.

[17] Y. Jiang, F. Wang, Z. Liu, and Z. Chen, "Composite learning adaptive tracking control for full-state constrained multiagent systems without using the feasibility condition," *IEEE Transactions on Neural Networks and Learning Systems*, 2022.

[18] Y. Shang, "Consensus tracking and containment in multiagent networks with state constraints," *IEEE Transactions on Systems, Man, and Cybernetics: Systems*, vol. 53, no. 3, pp. 1656–1665, 2022.

[19] P. Lin, Y. Wang, D. Wang, and Z. Wu, "Constrained containment control for multi-agent systems with possible empty intersection of position constraints," *IEEE Transactions on Automatic Control*, 2023.

[20] J. Á. Acosta, A. Dòria-Cerezo, and E. Fossas, "Diffeomorphism-based control of nonlinear systems subject to state constraints with actual applications," in *IEEE Conference on Control Applications*, 2014, pp. 923–928.

[21] D. Kurtoglu, T. Yucelen, and D. M. Tran, "Distributed control with time transformation: User-defined finite time convergence and beyond," in *AIAA SciTech 2022 Forum*, 2022, p. 1716.

[22] R. Kamalapurkar, J. A. Rosenfeld, A. Parikh, A. R. Teel, and W. E. Dixon, "Invariance-like results for nonautonomous switched systems," *IEEE Trans. on Automatic Control*, vol. 64, no. 2, pp. 614–627, 2018.